Journal for Geometry and Graphics
Volume 14 (2010), No. 2, 203–215.

Freeform Variations of Origami

Tomohiro Tachi

Graduate School of Arts and Sciences, The University of Tokyo
3-8-1 Komaba, Meguro-Ku, Tokyo 153-8902
email: tachi@idea.c.u-tokyo.ac.jp

Abstract. This paper presents a novel method to construct a 3D freeform surface that can be manufactured by folding a sheet of paper. More specifically, we provide a design system using which the user can intuitively vary a known origami pattern in 3D while preserving the developability and other optional conditions inherent in the original pattern. The system successfully provides 3D origami designs that have not been realized thus far.

Key Words: Origami, Developable Surface, Discrete Differential Geometry, Computer Aided Design.

MSC 2010: 53A05, 52B10, 52B70

1. Introduction

Origami is the art of folding, or more formally, isometrically transforming, a sheet of paper into various forms without stretching, cutting, or gluing another piece of paper to it. Using origami, a complex 3D shape can be produced with an isometric transformation; hence, it can be applied for forming the shapes of a variety of products, architectural elements, medical devices, and so on, with a watertight sheet of hard material so that there is no need to assemble multiple parts. In particular, the simultaneous kinetic motion of connected paper is potentially useful for assisting the manufacturing process and for realizing self-(re)configurable structures.

Several designs are proposed to produce 3D origami forms applicable in engineering contexts: e.g., polyhedral surfaces using periodic symmetry, such as *Miura-ori* [11], Resch's pattern [13], and *"waterbomb tessellation"* [4, 17]; and straight or curved developable surface reflected with respect to planes, such as Huffman's concentric circular tower (see [3]), Mosely's *"bud"* [12], and the extension of *Miura-ori* by Buri and Weinand [2]. However, the number of degrees of freedom of the shapes that can be produced using these designs is strictly limited because of the symmetry used in the design approach; this makes it impossible to freely control the resulting 3D shape.

When applying origami to actual designs for various applications including space structures, architectural structures and facades, medical devices, and other products in civil use,

ISSN 1433-8157/$ 2.50

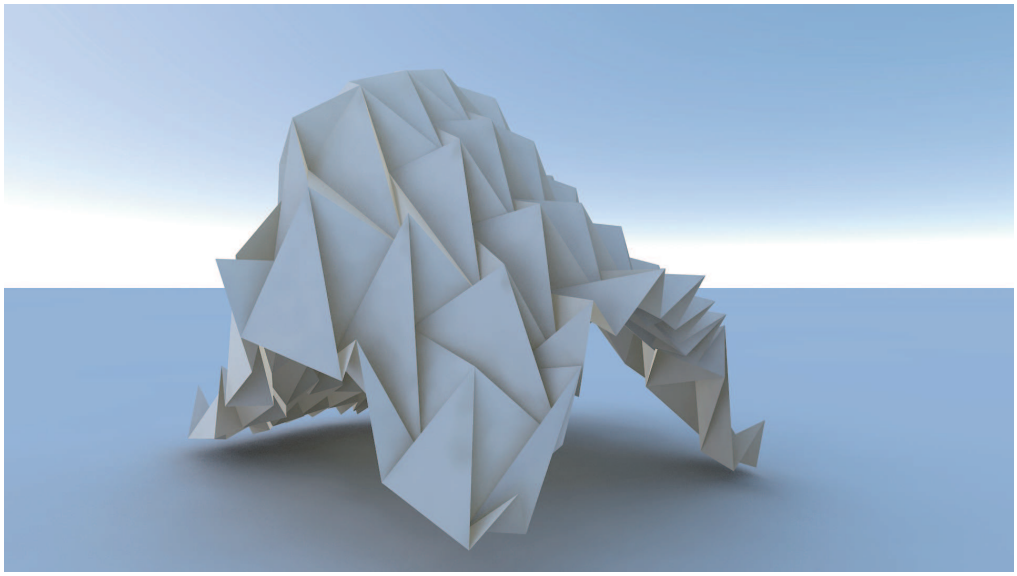

Figure 1: Example of freeform variations of origami

it is important to control the customized 3D shape in the resulting folded state so that the shape is consistent with the required functionality, existing structures, and environments. Therefore, computationally constructing an arbitrarily formed 3D surface using origami is a significant challenge not only to origami artists but also the engineers, designers, and personal users who apply origami to practical purposes.

The most generalized approach to realize an arbitrary 3D origami form is to use the *"Origamizer"* algorithm [16], which provides a crease pattern that folds into a given polyhedron. However, this method produces highly complex patterns comprising an interlocking structure by crimp folds; in this method, the crimp folds are necessary to exactly align the surface onto an arbitrarily tessellated polyhedral surface. This does not allow a continuous folding motion from a planar state to a 3D state; this becomes a significant disadvantage in applications to industrial manufacturing processes.

Our objective is to realize an easily foldable freeform surface manufactured from a sheet material. Although the generalization method proposed by the author [15] produces a variety of non-symmetric forms with valid folding motion, with this method, the topology of the foldline network was not controllable and only generalized Miura-ori design within a certain range of deformation can be produced. We extend this perturbation-based method so that it is possible to design various shapes by modifying and reconfiguring multiple origami patterns while preserving the conditions inherent in the original patterns (Fig. 1).

2. Geometric model of origami

An origami surface is a surface with creases characterized by the existence of a one-to-one isometric mapping between the flat and the 3D states. We model such a surface as a 3D piecewise linear surface under various geometric constraints so that an isometric mapping to a valid planar figure exists. The configuration is represented by the vertex coordinates $\mathbf{x}$ (where $\mathbf{x}$ is a $3n_{\text{vert}}$ vector and n_{vert} the number of vertices) of a triangular mesh whose edges represent creases assigned with a target folding angle of $-\pi$ (valley fold), 0 (3D crease), or π (mountain fold). (Note that in origami, folding angles $-\pi$ and π are different. In

the implementation software, the previous rotation angle value of each edge is stored for each frame and is used to determine the plausible angle from the candidates calculated from the vertex coordinates.) These variables are constrained by origami conditions including developability, which is a necessary condition to consist origami, and flat-foldability, which although not always necessary, is a basic condition shared by many origami designs. In addition, there are several design-specific conditions related to the coincident positions of elements of surfaces in the 3D and flat states. Therefore, we generalize origami patterns by flexibly changing the mesh configuration while ensuring that the sets of conditions inherent in the original patterns, i.e., the preserved features, are satisfied.

2.1. Developability

An *origami* is a developable surface with G^1 discontinuity whose most simple case is a polyhedral surface. As the curvature of a polyhedral surface cannot be defined, the developability of origami is given by zero Gauss area G_k around every interior vertex k:

$$G_k = 2\pi - \sum_i \theta_{k,i} = 0, \tag{1}$$

where $\theta_{k,i}$ is the i-th incident sector angle of vertex k. This discretized representation allows for more flexible variations of form than possible with a smooth developable surface, which is fundamentally a plane, cylinder, cone, or tangent surface.

2.2. Paper boundary

Traditionally, an origami is folded from a square or a fixed convex polygon. As the shape of the paper is not preserved by (1), we require additional conditions to be defined for the perimeter. This is represented as follows: For each vertex k on the perimeter,

$$\sum_i \theta_{k,i} - \sum_i \theta^0_{k,i} = 0, \tag{2}$$

and for every straight element j of the perimeter comprising edges i of length $\ell_{j,i}$,

$$\sum_i \ell_{j,i} - \sum_i \ell^0_{j,i} = 0, \tag{3}$$

where $\theta^0_{k,i}$ is the original incident sector angle of vertex k, and $\ell^0_{j,i}$ is the original length of i. In an engineering sense, the boundary property is not always important. Hence, on the basis of the design context, we can ignore this condition or instead set up another condition such as the convexity of the boundary of the paper:

$$\sum_i \theta_{k,i} \leq \pi\,. \tag{4}$$

2.3. Flat-foldability

Several origami models such as *Miura-ori*, *Yoshimura pattern*, and *waterbomb tessellation* are foldable to another flat state with every foldline folded completely, i.e., by $\pm\pi$. This condition is called *flat-foldability*, and it can be applied to design objects and spaces that can be compactly packed. Flat-foldability of origami can be represented as a combination of two

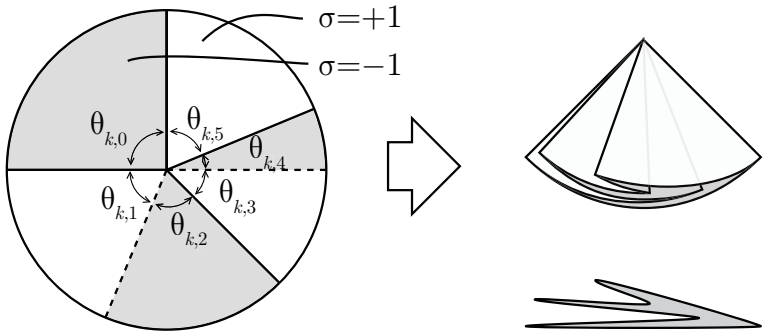

Figure 2: Flat-foldable vertex.

conditions — that the coordinates are valid and that a valid overlapping ordering exists. The former condition implies that there exists a valid isometric mapping to a plane and that this condition can be represented locally as follows: For each interior vertex k,

$$F_k = \sum_i \sigma_{k,i}\theta_{k,i} = 0, \tag{5}$$

where is $\sigma_{k,i} = \pm 1$ is the sign assigned to each facet representing the orientation of the facet in the flat-folded state (Fig. 2).

The order of overlap of surfaces must also be considered because multiple facets are mapped onto the same position in the plane when the surface is flat-folded. There have been several studies on this topic. Bern and Hayes [1] proved that determining a valid ordering from a crease pattern is an NP-complete problem with worst-case complexity. A practical exact algorithm is investigated by Meguro [10] that implements a divide-and-conquer approach to solve the overlapping problem in a practical amount of time for most well-designed origami. Although these exact approaches help us determine whether the given set of foldlines is valid, they provide no information for establishing valid foldlines. Therefore, our method uses angular inequalities that approximately remove local intersections: For four adjacent crease lines ℓ_{i-1}, ℓ_i, ℓ_{i+1}, and ℓ_{i+2}, where the two creases in the middle, ℓ_i and ℓ_{i+1}, have the same mountain-valley (MV) assignment (let us say that it is M without loss of generality). The sector angles between them, θ_{i-1}, θ_i, and θ_{i+1} (Fig. 3), satisfy the following:

$$\theta_i \geq \min(\theta_{i-1}, \theta_{i+1}), \tag{6}$$

additionally, if ℓ_{i-1}'s assigment is V,

$$\theta_i \geq \theta_{i-1} \tag{7}$$

and if ℓ_{i+2}'s assigment is V,

$$\theta_i \geq \theta_{i+1} \tag{8}$$

It should be noted that (6) is the necessary condition for flat-folding derived by Kawasaki [6] and that (7,8) is an empirical condition applicable to finding a locally closed vertex [14].

2.4. Folding angle conditions

To avoid a local collision between adjacent facets, the folding angle ρ (where, $|\rho| = \pi -$ *dihedral angle*) between each pair of adjacent facets must be maintained in the range $[-\pi, \pi]$. More specifically, the range of possible rotation angles is defined by the target rotation angle of the edge.

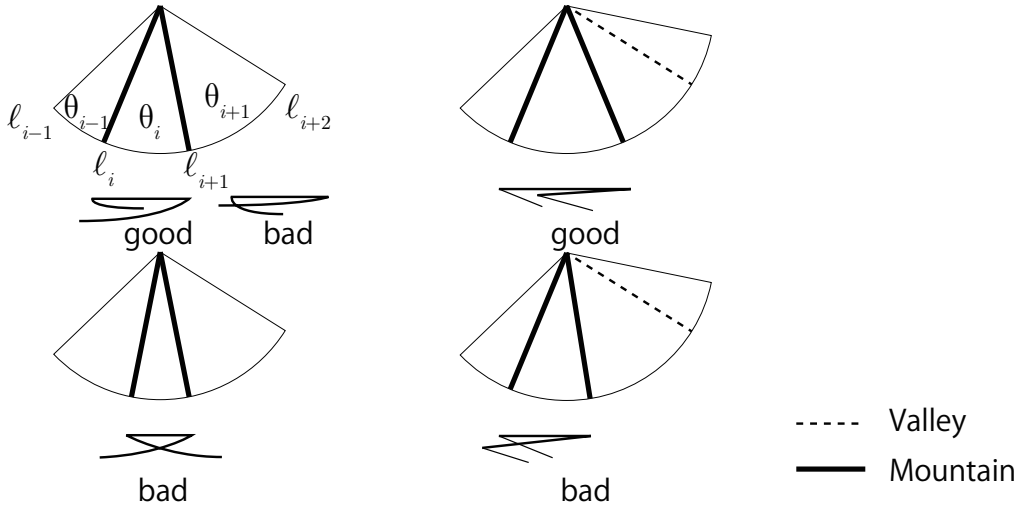

Figure 3: Angular inequalities for flat-foldability. Left: KAWASAKI's necessary condition. Right: an empirical condition.

1. If target is π, $0 \leq \rho \leq \pi$.
2. If target is $-\pi$, $-\pi \leq \rho \leq 0$.
3. If target is 0, $-\alpha\pi \leq \rho \leq \alpha\pi$ $(0 \leq \alpha < 1.0)$.

The first two conditions ensure that the fold is not made in the opposite direction as in the flat-folded state. This is important as creases cannot correct their orientation in a smooth folding process. The third condition is applied for the extra crease necessary to triangulate each facet surrounded by more than three creases. The folding angle of such a crease represents the twist of the facet element. The inequality is set up to make the surface practically feasible. Note that α $(0 \leq \alpha < 1.0)$ determines the flexibility of the paper in use (if 0, each facet is rigid and cannot twist).

3. Valid deformation

The given constraints are calculated numerically by iteratively solving linear equations. The process is an extension of the Newton-Raphson method, where solving $f(\mathbf{x}) = 0$ and $g(\mathbf{x}) \leq 0$ is understood as minimizing the respective penalty functions $f(\mathbf{x})^2$ and $\max(g(\mathbf{x}), 0)^2$. By combining the required conditions into one vector equation, we can obtain the form of $\mathbf{F}(\mathbf{x}) = \mathbf{0}$ for each step of the calculation.

As the number of constraints n_c is lower than the number of variables $3n_{\text{vert}}$ in origami models, the vector equation forms an under-constrained system; therefore, the solution is not fixed to one configuration. In order to solve this system, we use a method that modifies a known pattern that satisfies $\mathbf{F}(\mathbf{x}) = \mathbf{0}$, such as *Miura-ori* and *Resch's pattern*, by numerically integrating an infinitesimal deformation of a triangular mesh within the solution space of the equation

$$\left[\frac{\partial \mathbf{F}}{\partial \mathbf{x}}\right] d\mathbf{x} = \mathbf{0}\,, \tag{9}$$

where the $n_c \times 3n_{\text{vert}}$ rectangular matrix $[\partial \mathbf{F}/\partial \mathbf{x}]$ is the Jacobian matrix of the constraints. The infinitesimal deformation $d\mathbf{x}$ that satisfies is calculated using its pseudo-inverse (i.e.,

Penrose-Moore generalized inverse) $[\partial \mathbf{F}/\partial \mathbf{x}]^+$.

$$d\mathbf{x} = \left(\mathbf{I} - \left[\frac{\partial \mathbf{F}}{\partial \mathbf{x}} \right]^+ \left[\frac{\partial \mathbf{F}}{\partial \mathbf{x}} \right] \right) d\mathbf{x}_0 \,, \tag{10}$$

where $d\mathbf{x}_0$ is an arbitrarily given deformation vector. Note that the typical conditions are linearly expressed in terms of the sector angles $\boldsymbol{\theta}$ and folding angles $\boldsymbol{\rho}$ in the pattern. We can use the following form:

$$\left[\frac{\partial \mathbf{F}}{\partial \mathbf{x}} \right] = \left[\frac{\partial \mathbf{F}}{\partial \boldsymbol{\theta}} \right] \left[\frac{\partial \boldsymbol{\theta}}{\partial \mathbf{x}} \right] + \left[\frac{\partial \mathbf{F}}{\partial \boldsymbol{\rho}} \right] \left[\frac{\partial \boldsymbol{\rho}}{\partial \mathbf{x}} \right] , \tag{11}$$

where the elements of $[\partial \boldsymbol{\theta}/\partial \mathbf{x}]$ and $[\partial \boldsymbol{\rho}/\partial \mathbf{x}]$ are represented as follows. As in Fig. 4, the angle and the normal of the triangle ijk (the coordinates are denoted as $\mathbf{x}_i$, $\mathbf{x}_j$, and $\mathbf{x}_k$, respectively) are denoted as $\theta_{j,ki}$ and $\mathbf{n}_{ijk}$, respectively, and the folding angle of ji and the length of the perpendicular from k to ji are denoted as ρ_{ij} and $h_{k,ij}$, respectively. We get,

$$\frac{\partial \theta_{j,ki}}{\partial \mathbf{x}_i} = \frac{\mathbf{n}_{ijk} \times (\mathbf{x}_i - \mathbf{x}_j)}{\|\mathbf{x}_i - \mathbf{x}_j\|^2}, \tag{12}$$

$$\frac{\partial \theta_{j,ki}}{\partial \mathbf{x}_j} = -\frac{\mathbf{n}_{ijk} \times (\mathbf{x}_i - \mathbf{x}_j)}{\|\mathbf{x}_i - \mathbf{x}_j\|^2} + \frac{\mathbf{n}_{ijk} \times (\mathbf{x}_k - \mathbf{x}_j)}{\|\mathbf{x}_k - \mathbf{x}_j\|^2}, \tag{13}$$

$$\frac{\partial \theta_{j,ki}}{\partial \mathbf{x}_k} = -\frac{\mathbf{n}_{ijk} \times (\mathbf{x}_k - \mathbf{x}_j)}{\|\mathbf{x}_k - \mathbf{x}_j\|^2}; \tag{14}$$

and

$$\frac{\partial \rho_{ij}}{\partial \mathbf{x}_k} = \frac{\mathbf{n}_{ijk}}{h_{k,ij}}, \tag{15}$$

$$\frac{\partial \rho_{ij}}{\partial \mathbf{x}_l} = \frac{\mathbf{n}_{jil}}{h_{l,ij}}, \tag{16}$$

$$\frac{\partial \rho_{ij}}{\partial \mathbf{x}_i} = \frac{-\cot \theta_{j,ki}}{\cot \theta_{j,ki} + \cot \theta_{i,jk}} \frac{\mathbf{n}_{ijk}}{h_{k,ij}} + \frac{-\cot \theta_{j,il}}{\cot \theta_{j,il} + \cot \theta_{i,lj}} \frac{\mathbf{n}_{jil}}{h_{l,ij}}, \tag{17}$$

$$\frac{\partial \rho_{ij}}{\partial \mathbf{x}_j} = \frac{-\cot \theta_{i,jk}}{\cot \theta_{j,ki} + \cot \theta_{i,jk}} \frac{\mathbf{n}_{ijk}}{h_{k,ij}} + \frac{-\cot \theta_{i,lj}}{\cot \theta_{j,il} + \cot \theta_{i,lj}} \frac{\mathbf{n}_{jil}}{h_{l,ij}}. \tag{18}$$

The vertex coordinates are deformed along $d\mathbf{x}$, which is the valid deformation closest to estimated deformation $d\mathbf{x}_0$. Since $d\mathbf{x}_0$ can be specified arbitrarily, we can use a user input of direct dragging of the surface in 3D to construct the vector. The solution is calculated using Euler integration. A step of the Newton-Raphson method is applied to each integration step to numerically eliminate residual error caused by nonlinear and inequality conditions.

4. Mesh modification

When we deform the surface by a large amount, the pattern transforms such that vertices can no longer traverse along the surface because of the intersection of the surrounding edges. This limits the amount of deformation that the surface can tolerate, and it is necessary to reconfigure the mesh structure to achieve further deformation. Such limited deformation of the mesh structure is detected by the presence of degenerated edges. For each edge that is too short, an operation similar to the edge collapse operation proposed by Hoppe et al. [5]

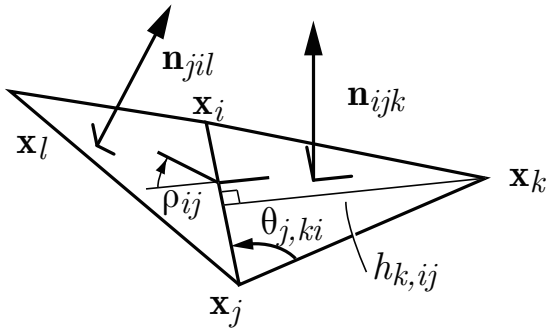

Figure 4: Notation used for defining elements of $[\partial\boldsymbol{\theta}/\partial\mathbf{x}]$ and $[\partial\boldsymbol{\rho}/\partial\mathbf{x}]$.

is performed. When the flat-foldability of the original pattern is to be preserved, the process must take into account the target folding angles assigned to the creases. The following are the rules that must be followed during the collapsing process to keep the configuration of the flat-folded state unchanged.

- When two edges are merged into one, the target angle for the merged edge is the sum of the original target angles.
- The sum of the target angles around the merged vertex must be -2π (convex) or 2π (concave) (Maekawa's theorem [9]).
- A minimum of four creases should surround each interior vertex.

Therefore, the possible merging processes are limited to the following two cases (double signs correspond respectively):

1. Vertices with sum of angles $\pm 2\pi$ and $\pm 2\pi$ are merged by collapsing a $\pm\pi$ edge, forming a $\pm 2\pi$ vertex.
2. Vertices with sum of angles 2π and -2π are merged by collapsing a $\pm\pi$ edge, forming a $\mp 2\pi$ vertex.

In most mesh optimization techniques, edge flipping is used along with edge collapse to avoid the formation of a jagged surface. However, our method applies this procedure only to creases that must remain unfolded throughout the folding motion (when target angle is 0 and $\alpha = 0$) given that nonsmooth small creases play an important role in origami. In other words, the variety of forms possible with origami originates in the G^1 discontinuity of the surface. The above described mesh modification process significantly changes the topology of the crease pattern structure of origami; this results in the creation of a new origami pattern that combines different types of vertices (Fig. 7, Right).

5. Implementation

We propose a system to explore the variations of origami forms through an interactive user interface that enables the user to freely drag the vertices of a surface in a folded 3D state while the system calculates the geometric constraints in the background. While editing, the user can see the crease pattern and the flat-folded pattern (if the model is flat-foldable). In addition, the user can switch between the design and edit modes: in the design mode, features in the design context are preserved; whereas in the simulation mode, preserves the length of the elements of the paper and simulates how the designed paper behaves.

The system is implemented in C++ using wxWidgets and OpenGL for the graphical interface and BLAS (Intel MKL) for numerical calculations. The system completes the iterated

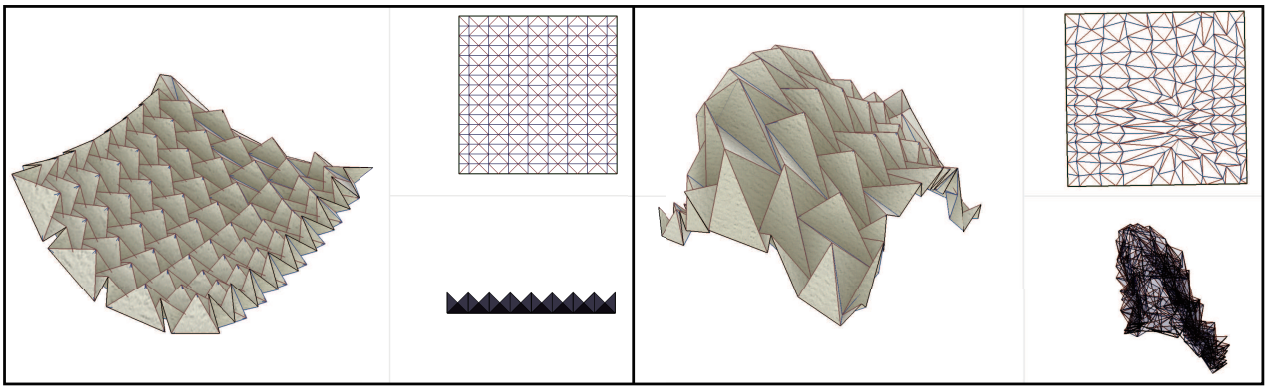

Figure 5: Variations of *waterbomb tessellation*. Left: regular pattern. Right: deformed pattern forming a double-curved surface. For each figure, left: 3D form, upper-right: crease pattern, bottom-right: flat-folded pattern.

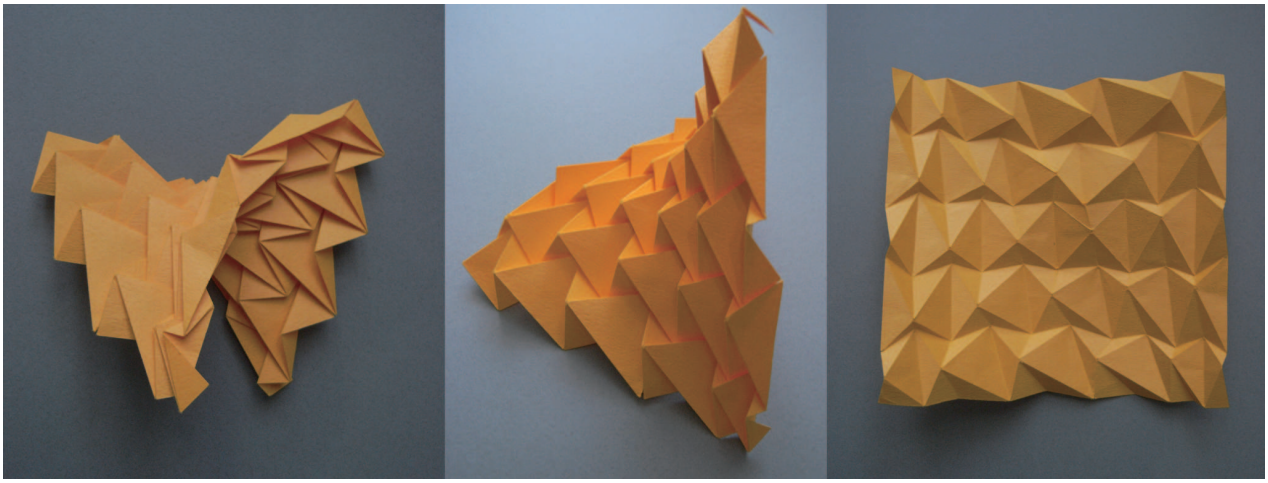

Figure 6: Folded model of a variation of the *waterbomb tessellation*. Left: flat-folded state. Center: 3D state. Right: the developed state.

step of equation (10) via the conjugate gradient method (number of iterations is limited to 512 for each frame) at 1-5 fps for a 256 vertex model with 452 constraints on a laptop PC with a quad-core processor (Intel Core i7 1.6 GHz).

6. Model examples and results

An appropriate set of origami conditions enables the generalization of various known origami tessellation patterns. Here, we show actual examples of generalized origami patterns.

6.1. Waterbomb tessellation

The *waterbomb tessellation* is a triangle-based flat-foldable pattern folded into a cylindrical surface. This pattern is well-known to various origami artists, one of the earliest design using which is by Fujimoto [4], and it is also applied for deployable structures such as a stent graft [16]. The curvature of the surface can be altered by varying the pattern using our method (Fig. 5). As the surface is composed of both convex and concave vertices, the

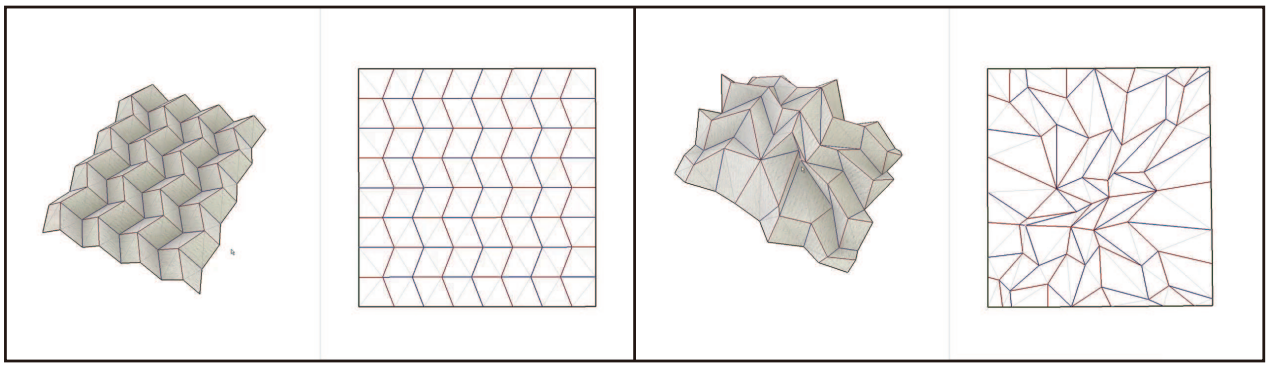

Figure 7: Variations of *Miura-ori*. Left: regular *Miura-ori*. Right: deformed pattern. Notice the topological change in the crease pattern network.

Figure 8: Variation of *Yoshimura pattern*

resulting generalized pattern is flexible enough to enable the creation of origami forms that approximate a 3D freeform surface.

The resulting models were constructed by folding a sheet of paper whose surface was scored with a CNC cutting plotter (Fig. 6). Although a certain level of folding skill is still required to construct this pattern, it is observed that the pattern can collapse into the folded state once we have the right precreases on the surface. This hints at the possibility of the development of an automated manufacturing method in the future.

6.2. Miura-ori

Miura-ori [11] is a quadrilateral-based flat-foldable pattern folded into a 3D corrugated surface that approximately follows the shape of a plane. Figure 7 shows an example of this design. In this example, we have applied boundary condition (2) and used $\alpha = 0.1$ for each triangulating crease to approximate the surface's elastic feature.

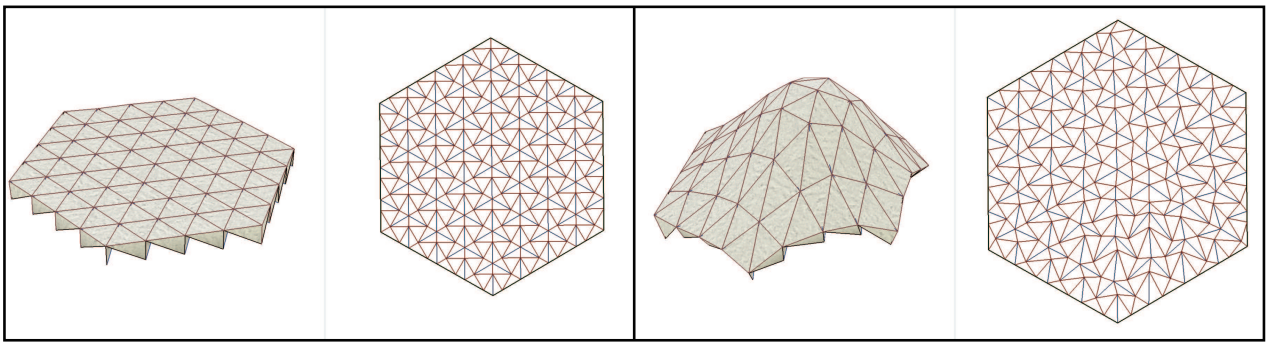

Figure 9: A variation of *Resch's triangular pattern*. Left: Original pattern. Right: A variation forming a double-curved polyhedral triangular mesh.

6.3. Yoshimura pattern

The *Yoshimura pattern* is a triangular (diamond) flat-foldable pattern that folds into a cylindrical surface (see [11]). As all vertices are convex and cannot be altered by our mesh modification method, the approximate mean curvature of the surface is always positive. Hence, although we can produce many variations of the *Yoshimura pattern*, its very topology significantly limits the scope for variation. Figure 8 shows a rendering of a freeform shell using the deformation of the *Yoshimura pattern*.

6.4. Resch's triangular pattern

The triangular tessellation proposed by Resch [13] is a developable and non flat-foldable surface in which a group of three vertices forms a vertex in the folded form to hide a tuck-like flat-folded part behind a composed plane. This type of coincidence of points is calculated by adding extra constraints or removing the variables and combining the equations incident at the vertices. The variational patterns form polyhedral surfaces with tucks folded behind. This can be interpreted as a special case of origamizer method [16], where in our method,

Figure 10: Design of crumpled paper

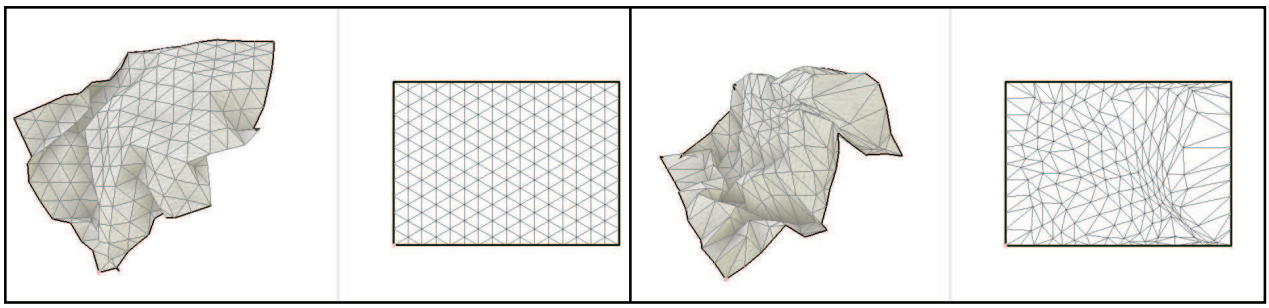

Figure 11: Left: Isometric triangular grid.
Right: Irregular developable surface with fixed boundary.

the pattern works without crimp folding. While the variation, we do not allow the surface to change the topology of the crease pattern in order to retain the characteristics of the pattern that forms a polyhedral surface.

6.5. Plane (crumpled paper)

Transforming a planar paper, i.e., a regular triangular mesh without a crease, results in the formation of an irregularly corrugated surface or, put simply, crumpled paper. Hence, our method can also be used for designing and rendering crumpled paper (Fig. 10), and we found that it yields better results than directly simulating the non-stretching behavior of a sheet of paper; the latter tends to produce visible regular triangular artifacts (Fig. 11).

6.6. Curved folding

We further tested applying the method to designing curved folds. As demonstrated by Liu et al. [8] and Kilian et al. [7], a smooth developable patch, i.e., a torsion-free ruled surface, between creases can be approximated by a planar quadrilateral strip. Planar quadrilaterals can be formed by a triangular mesh with creases whose target folding angle is 0 and $\alpha = 0$. We were able to obtain nonsymmetric curved folding shapes by carefully transforming a regular rectangular grid, but it was found that the surface can easily become jagged (Fig. 12). The problem arises because of the excess degrees of freedom in the configuration. To solve this problem, studies must be conducted on the addition of more constraints to the system to preserve the smoothness of the continuous foldlines and the surface.

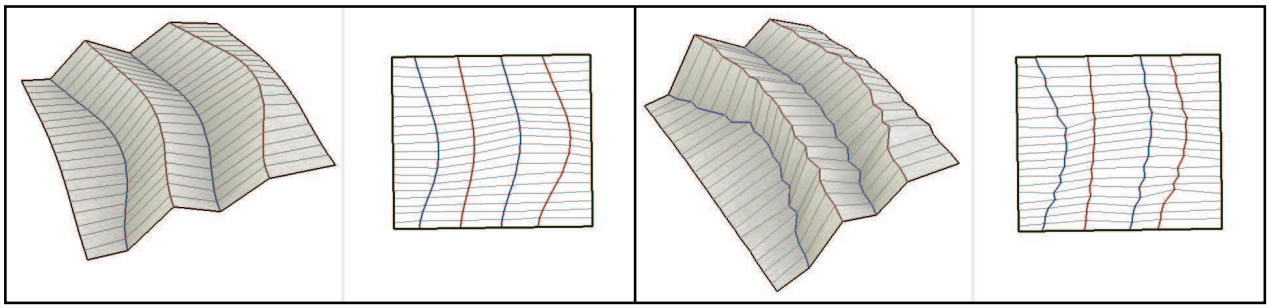

Figure 12: Designing curved folding. Top: good curved folding. Bottom: a jagged surface

7. Conclusion and future work

This paper described a novel method for obtaining a generalized form of origami model by numerically integrating infinitesimal deformations under origami constraints and collapsing edges to alter the topology of the crease pattern. The method enables the realization of new and complex origami patterns that are not achievable with existing design methods. We have developed a system that implements the proposed method (the software is available from the author's web site[1]). Certain features of the original origami patterns, such as foldability from a plane, flat-foldability, and the smooth transformation from one state to another, can also be preserved in the designed models if the user so desires. The system can be used for different applications by choosing different sets of active conditions.

A future work of this study is in developing a method that fully support curved folding. In addition, whereas in this study the topology of the surface is limited only to a that of a disk, future studies for extending the method to nondisk surfaces, especially cylindrical surfaces, can widen the field of possible applications of origami designs; examples of such applications include collapsible containers and portable architectural spaces.

Acknowledgment

This study is supported by the grant in aid for JSPS fellows and by KAKENHI (22800009) Grant-in-Aid for Research Activity Start-up, by Japan Society for the Promotion of Science.

References

[1] M. Bern, B. Hayes: *The complexity of flat origami*. Proc. 7th Annual ACM-SIAM Symposium on Discrete Algorithms 1996, pp. 175–183.

[2] H. Buri, Y. Weinand: *ORIGAMI – Folded Plate Structures, Architecture*. 10th World Conference on Timber Engineering, 2008.

[3] E. Demaine, M. Demaine: *History of Curved Origami Sculpture*. `http://erikdemaine.org/curved/history/`.

[4] S. Fujimoto: *"Souzousei wo kaihatsu suru rittai origami"* [in Japanese]. Hyougo-ken Gakkou Kouseikai Tamba Shibu 1976.

[5] H. Hoppe, T. DeRose, T. Duchamp, J. McDonald, W. Stuetzle: *Mesh optimization*. Proc. ACM SIGGRAPH 1993, pp. 19–26.

[6] T. Kawasaki: *On the relation between mountain-creases and valley-creases of a flat origami*. Proc. 1st Internat. Meeting of Origami Science and Technology 1989, pp. 229–237.

[7] M. Kilian, S. Flöry, N.J. Mitra, H. Pottmann: *Curved folding*. ACM Transactions on Graphics **27**(3), 1–9 (2008), Proc. of SIGGRAPH 2008.

[8] Y. Liu, H. Pottmann, J. Wallner, Y.-L. Yang, W. Wang: *Geometric modeling with conical meshes and developable surfaces*. ACM Transactions on Graphics **25**(3), 681–689 (2006).

[9] J. Maekawa: *VIVA! Origami*. Sanrio 1983.

[10] T. Meguro: *Orihime*. `http://www.geocities.co.jp/HeartLand-Oak/5487/`, 2008.

[1] `http://www.tsg.ne.jp/TT/software/`

[11] K. Miura: *Proposition of pseudo-cylindrical concave polyhedral shells*. Proc. of IASS Symposium on Folded Plates and Prismatic Structures, 1970.

[12] J. Mosely: *Curved origami*. SIGGRAPH 2008 Electronic Art and Animation Catalog, pp. 60–61.

[13] R. Resch, H. Christiansen: *he design and analysis of kinematic folded plate systems*. Proc. IASS Symposium on Folded Plates and Prismatic Structures, 1970.

[14] T. Tachi: *Smooth origami animation by crease line adjustment*. ACM SIGGRAPH 2006 Posters.

[15] T. Tachi: *Generalization of rigid-foldable quadrilateral-mesh origami*. Journal of the International Association for Shell and Spatial Structures **50**(3), 173–179 (2009).

[16] T. Tachi: *Origamizing polyhedral surfaces*. IEEE Transactions on Visualization and Computer Graphics **16**(2), 298–311 (2010).

[17] Z. You, K. Kuribayashi: *A novel origami stent*. Proc. 2003 Summer Bioengineering Conference, pp. 257–258.

Received August 7, 2010; final form November 24, 2010